JOURNAL OF COMPUTATIONAL PHYSICS 23, 1–22 (1977)

Higher Order Monotonic Convective Difference Schemes

C. K. FORESTER

Boeing Commercial Airplane Company, Seattle, Washington 98124

Received June 6, 1975; revised January 19, 1976

Eulerian mesh computations of simple linear and nonlinear one-dimensional wave propagations with second and higher order convective difference schemes exhibit nonphysical oscillations near steep gradient regions of the solution. This computational noise may propagate a significant number of mesh intervals away from the regions in which it is generated and severely compromise the solution accuracy. Boris, Book, and van Leer have developed nonlinear filtering techniques for second order convection algorithms which effectively remove computational noise from steep gradient solutions. The principal disadvantage of these filtering techniques is that solutions of sharply peaked waves are penalized in amplitude accuracy of the extrema. A nonlinear method of filtering computational noise from fourth and higher order accurate convective difference schemes is introduced which removes the computational noise without inflicting significant amplitude losses in sharply peaked waves. One-dimensional simple linear and nonlinear test problems are used to illustrate the performance of various unfiltered and filtered convective difference schemes. It is noted that the filtered higher order convective difference schemes require less than one-third of the mesh points of the filtered second order convective difference schemes to model the extrema of sharply peaked waves to the same accuracy.

Finally, the Accurate Space Derivative method of Gazdag is shown to function with the global numerical differentiation performed with compact polynomial splines. This method is at least sixth and tenth order accurate, respectively, for modeling linear waves with cubic and quintic spline differentation for Courant numbers less than about $\frac{1}{4}$.

1. INTRODUCTION

Various convective difference schemes are available for approximating the convective equations of fluid dynamics. The first order accurate schemes may be the most dependable in providing solutions which are free of computational noise but these schemes are not the most cost effective to use in many cases. As a consequence, the development of higher order accurate convective difference schemes has continued. Some examples of these approximations are given in [1–5].

All of these higher order approximation methods possess the peculiar property that nonphysical oscillations in the solution can be generated in the vicinity of steep gradient regions. This computational noise may degrade or destroy the solution accuracy. Undesirable physical features of the simulated flow such as

ISSN 0021-9991

negative mass or energy densities may develop. In two or three space dimensions, additional undesirable physical features of the simulated flow such as spurious vortices may also develop. An example of the latter difficulty is now cited.

Fromm and Harlow [6] excited the interest of many people in numerical fluid mechanics with the numerically generated vortex-shedding photographs for simulated incompressible flow about rectangular cylinders. In the stagnation region upstream of the obstacle corners, the computations were troubled with numerical noise with a wavelength of two mesh intervals. This author repeated some of these computations with a Crank–Nicholson type of time differencing with second order space differencing in a staggered mesh arrangement of the type used by Fromm and Harlow [6] with the pressure defined in the center of the velocity cluster. The incompressible Navier–Stokes equations were used rather than the vorticity stream-function approach. A Poisson equation of the pressure field was used to ensure mass conservation [7]. After the simulation is begun from a slightly perturbed potential flow solution, computational noise was observed as cyclical vortex shedding which develops *upstream* of the obstacle corners. The usual Karman vortex street is almost completely disfigured with these vortices on the length scale of two to three mesh intervals. These vortex shedding computations were also performed with the convective terms modeled with the MacCormack [2] differencing. For Courant numbers, $\sigma = |u|(\Delta t)/\Delta x$, less than about $\frac{1}{2}$, computational noise was again observed in a manner similar to that for the model with the Crank–Nicholson time differencing. For simulations at Courant numbers greater than $\frac{1}{2}$, the usual Karman vortex street was computed free of the spurious vortices with results similar to those given by Fromm and Harlow [6]. At these Courant numbers, the dissipative properties of the MacCormack differencing provided enough artificial diffusion to eradicate the computational noise from the solutions. The spurious vortices can also be eradicated from these solutions by mesh refinement, which ensures that the cell Reynolds number is less than approximately 1. There are situations in flow computations at practical Reynolds numbers in which the dissipative properties of a difference scheme may be insufficient to adequately control computational noise (see, for example, [8]). Moreover, mesh refinement to ensure that the computational cell Reynolds numbers are of the order of unity may not be feasible for reasons of economics. In these cases, it is most cost effective to apply a smoothing technique to the solution procedure to remove the worst consequences of computational noise. There are many examples in the open literature of solutions which are adversely affected by computational noise and of techniques for removing this noise. No attempt is made to compare all of these smoothing techniques. Rather, it is the purpose of this paper to introduce a general purpose type of filtering technique and compare its performance to the following two filters for second order convective difference schemes.

Boris and Book [9, 10] and van Leer [11] have introduced two approaches to the design of filtered second order schemes. These algorithms substantially inhibit or eliminate computational noise generated in strong gradient regions by using nonlinear smoothing techniques. These filtered convective algorithms are called monotonic schemes because they yield single dependent variable solutions in which the solutions are monotonic between the desirable physical extrema without nonphysical accentuation of these extrema. In the case of coupled multiple-variable simulations, these algorithms may not completely eradicate the computational noise near steep gradients but the filters prevent the noise from being radiated many mesh points from the steep gradient regions. See, for example, [9]. For the purposes of illustrating the design and performance of the proposed filter in conjunction with fourth and higher order convective difference methods, the discrete solution of the hyperbolic equation

$$(\partial\omega/\partial t) + (\partial(u\omega)/\partial x) = 0 \tag{1}$$

is used for cases where u equals 1 and where u equals $\omega/2$ for several different initial conditions. The noise waves normally generated by the finite difference approximations to Eq. (1) are suppressed with a nonlinear filter which locally transforms Eq. (1) into

$$(\partial\omega/\partial t) + (\partial(u\omega)/\partial x) = (\partial/\partial x)(\mu\, \partial\omega/\partial x) \tag{2}$$

only in the regions where the noise waves are generated and propagated.

This is the reverse of the procedure presented by Boris and Book [9, 10] in which the finite difference approximation of the right-hand term of Eq. (2) is added into the algorithm of Eq. (1) at every mesh point and then it may be subtracted out after the solution is advanced a time step when certain criteria are satisfies. The *reversible*[1] version of the *Boris–Book* algorithm [10] is used in the test calculations which employs Crank–Nicholson time differencing with second order space differencing and a viscous coefficient which is a function of the Courant number. The reversible Boris–Book algorithm yields single-variable monotonic solutions for Courant numbers less than about 0.6. By setting the viscous coefficient equal to 0.13 for Courant numbers greater than 0.6, stable but not monotonic computations are achieved up to a Courant number of unity in the solution of linear problems.

Van Leer [11] has presented a method of integrating Eq. (1) which achieves monotonic solutions in steep gradient regions through the addition of a nonlinear third order term tailored to the second order "zero-average-phase-error method"

[1] The italicized words are used in the illustrations of Section 3 to identify the convective algorithm applied to the test problems.

of Fromm [12]. The method referred to as the *Fromm monotonic* scheme is monotonic for Courant numbers less than or equal to 1.

Other second order convective difference schemes examined include the *Leith* (see [12]) scheme (to which the Lax–Wendroff schemes reduce for linear problems) and the *upstream* version of Leith's scheme by *Fromm* [12]. The second order "zero-average-phase-error method" is constructed by averaging these schemes. The second order Crank–Nicholson scheme behaves like Leith's scheme at small Courant numbers. Unlike the Leith scheme, however, it has no damping of lagging-error-waves as the Courant number is raised toward 1. As a consequence, it was the noisiest second order algorithm tested.

The fourth order methods examined include a *spatial fourth* approximation (see, for example, [13]) with Crank–Nicholson time differencing, *Crowley fourth* [14], the *one-flux Fromm* [15] scheme, and the *two-flux Fromm* [16] scheme. (These two schemes presented by Fromm are nonlinear conservative variants of the Crowley [14] scheme.)

Other higher order schemes were examined which included *spatial sixth* and *eighth* order approximations with Crank–Nicholson time differencing, and the Accurate Space Derivative (ASD) method of Gazdag [5] with the global numerical differentiation performed with *cubic* (third degree), *quintic* (fifth degree), or *septemtic* (seventh degree) polynomial *splines* (herafter referred to as splines) rather than the truncated Fourier series which Gazdag used. Higher derivatives are obtained by splining the lower order derivatives. Thus, the first derivatives are obtained by splining the mesh function data. The second spatial derivatives are obtained by splining the first spatial derivatives. This process is repeated for spatial derivatives of any desired order. The symbols $P = 3$ *or* $P = 4$ used by Gazdag are used here in the same way to designate the number of terms which are retained in the timewise truncated Taylor expansion. Thus Gazdag's ASD method is only modified at the point by which the spatial derivatives are obtained.

The global differentiation by splines is implemented by the efficient explicit tridiagonal matrix algorithm [17] whose elements are matrices for splines of odd-degree five and above. For the cubic spline, only three multiples and nine fetches per mesh point are required to get a splined derivative at each mesh point. The only discrete datum required at each mesh point to implement the cubic spline is the centered difference expression $(A_{i+1} - A_{i-1})/(2\Delta x)$. For higher degree splines, the expression $(A_{i+1} - 2A_i + A_{i-1})/(\Delta x)/(\Delta x)$ is also required at each mesh point where (A) is the value of (ω) or derivatives of (ω). For the generation of the splined derivative at each mesh point, (A) is set to (ω) at each mesh point. For the generation of the second splined derivative at each mesh point, (A) is set to the first derivative of (ω) at each mesh point as supplied by the first splined differentation process. This process is repeated to the degree necessary to generate the required values of (A) at each mesh point.

For the generation of quintic splined derivatives, 15 multiples per mesh point are necessary. $(4((N-1)/2)^2+3)$ multiples per mesh point are required to implement a splined derivative for septemtic (seventh degree) and higher-odd-degree splines where (N) is the degree of the polynomial which is the basis function for the spline. Splines of discrete mesh function data yield directly the discrete $((N-1)/2)$ derivatives. A formula can be derived to relate the $((N-1)/2+1)$ derivative to the others directly available. For quintic and higher degree splines, the directly available higher derivatives can be used where appropriate rather than using spline-on-splines as defined above to get the needed derivatives. Computational costs of generating the derivatives can be reduced by this strategem with little loss in accuracy. As far as nonperiodic boundary conditions are concerned, $((N-1)/2)$ derivatives are required at the ends of the mesh. The values of the mesh function are also required at the ends of the mesh. For cubic splines, these conditions are straightforward to satisfy in a number of ways (see, for example, [18]). Further discussion of these choices is left to future studies. For the calculation reported herein, the derivatives required at the ends of the mesh are set to zero.

The order of accuracy in space offered by the splined ASD method is more than twice the value of (N) for linear problems with the Courant number less than about $\frac{1}{4}$ for any value of P greater than 2. Thus the cubic splined ASD and the quintic splined ASD methods are at least sixth and tenth order accurate in space at small Courant numbers for linear problems. For Courant numbers greater than about $\frac{1}{4}$, the order of accuracy of the splined ASD method is related to both (N) and (P). The quintic splined ASD solution has errors about midway between a spatial fourth order accurate difference approximation and the pseudospectral method compared by Orszag and Jayne [13] with finite difference approximations. Computations with the septemtic splined ASD method show further increase in accuracy over the quintic splined ASD method. Based on these results, it is expected that the nonatic (ninth) and higher-degree splined ASD method will provide accuracies approaching the pseudospectral or spectral methods.

This author computed the propagation of a plane two-dimensional inviscid incompressible vortex-pair in a quiescent inviscid environment with the previously mentioned second order method [7] which is mass and kinetic energy preserving. The vortex pair was defined as two identical counter rotating vortices in close proximity to one another whose mean direction of propagation was perpendicular to the line connecting the center of each vortex. The initial conditions for the mean propagation direction of the vortex pair were defined either at zero or 45 degrees to the coordinates of a square mesh of 28 by 28 computational cells. Several different vortex-pair sizes were used so that the sensitivity of the results to mesh size could be assessed. The results showed that the difference scheme propagated the vortex pair with much less loss in accuracy with the initial mean

direction of propagation at zero degrees than compared with 45 degrees to the mesh coordinates. Mesh refinement tended to reduce the severity of the wave propagation anisotropy, but not dramatically. Fromm [3] added approximations to 32 cross-derivative terms to a fourth order convective algorithm of two-dimensional unsteady incompressible flow to achieve stable fourth order accuracy and more nearly isotropic behavior of wave propagation diagonal to the mesh coordinates compared with wave propagation with the mesh coordinates.

The splined ASD method is a convenient means of generating approximations to all of these higher order cross-derivative terms which are needed to reduce the anisotropic diagonal flow errors. The splined ASD method has the further advantage that the user can flexibly choose the order of accuracy by the degree of the spline function selected. Additionally, the splined ASD method applies to arbitrary numbers of mesh points whereas methods dependent upon fast Fourier transforms do not. The attempt at the complex task of comparing the efficiency of the filtered splined ASD method with other discrete algorithms in useful computer programs is left to future studies.

The method of implementing the Crank–Nicholson time differencing in the *spatial fourth*, *spatial sixth*, *spatial eighth*, and *reversible Boris–Book* schemes is by iterating upon the implicit equations until the errors between successive iterations are reduced below some preselected low values. The iterative procedure is patterned after that used in [7]. Iteration is used to solve these equations because of the computer programming convenience offered.

The formulation of the smoothing routine for the fourth and higher order discrete approximations to Eq. (1) is presented in Section 2. The description of the comparative numerical experiments for several shapes of simple linear waves and two nonlinear waves for various values of the Courant number are presented in Section 3.

2. A Nonlinear Noise Filter

In this section, an iterative conservative smoothing process is defined which removes computational noise from convective computation of the dependent variable ω. The mesh function variables ϕ and S are assigned values for all values of (i) between 1 and mm where mm is the number of mesh points considered for the convective computation of the dependent variable ω. ϕ and S are variables necessary to the implementation of highly discriminate smoothing with the conservative numerical diffusion law

$$\omega_i^{k+1} = \omega_i{}^k + (\mu/2)(\Delta\omega_{i+1/2}(\phi_i + \phi_{i+1}) - \Delta\omega_{i-1/2}(\phi_i + \phi_{i-1}))^k, \tag{3}$$

where

$$\Delta\omega_{i-1/2} \equiv \omega_i - \omega_{i-1},$$
$$S_i \equiv (\Delta\omega)_{i-1/2}/|\Delta\omega_{i-1/2}|,$$
$$K \geqslant k \geqslant 1,$$
$$\mu < \tfrac{1}{2}.$$

ϕ is set to zero for all values of (i) except at certain mesh points at which ϕ is reset to 1. The criteria for defining the nonzero ϕ values are now presented.

Consider a typical interior mesh point removed $(n + 1)$ mesh intervals from the mesh boundary. S is computed for values of (i) equal to $(i - n)$ through $(i + 1 + n)$. If the signs of S_i and S_{i+1} are opposite, an extremum of ω_i is determined. At such a value of (i), S_i, S_{i-1}, S_{i-2},..., S_{i-n} are all required to have the same sign. Additionally S_{i+1}, S_{i+2}, S_{i+3},..., S_{i+1+n} are all required to have the same but opposite sign as the sign of S_i. If all of the signs of S are as required, sign continuity exists on each side of the extremum ω_i. Sign continuity is a mathematical way of determining the continuity of the slope of lines connecting values of ω assigned to adjoining mesh points on each side of ω_i. If slope or sign continuity does not prevail for (n) values of S on each side of the extremum in ω_i, ϕ is reset to 1 for the range of (i) from $(i - m)$ through $(i + m)$. No testing for sign continuity is performed unless ω_i is an extremum. The preceding sorting and labeling process is applied to each mesh point except near boundaries of the mesh, which must be treated in a special manner to prevent artificial diffusion of ω through the mesh boundary points. The method of treatment of the near boundary and boundary points is left to future studies.

To ensure that the strings of mesh points at which ϕ is nonzero in fact designate the regions of the mesh in which computational noise resides, it is necessary that the proper magnitudes of (n) and (m) be chosen for a particular convective algorithm. (n) represents one-half the wavelength of the noise waves with the greatest wavelength. The fundamental assumption about the noise properties of convective algorithms is that the noise of the longest wavelength occurs in the linear convective situation. Otherwise, the nonlinear effects in the general convective situation tend to drive the wavelengths of computational noise toward the limit of two mesh intervals. The magnitude of (m) simply must be large enough to permit the nonzero ϕ values to be continuous over any region in which the above sorting process defines a noise wave. If (n) is 2 or 3, it can be shown that (m) must be 1. If (n) is 4 or 5, it can be shown that (m) must be 2. As is shown in Section 3, values of (n) larger than 5 need not be considered for the fourth and higher order convective algorithms italicized in Section 1. In order to remove the computational noise from these convective algorithms, Eq. (3) together with the sign continuity logic and ϕ labeling procedure is iterated K times. When all values of ϕ are zero from this iterative conservative smoothing process, the resultant solutions of ω are defined as monotonic.

This definition of a monotonic solution is employed in the remainder of the discussion except where the term "nearly monotonic" is referred to. The latter term means that the solution is permitted to exhibit overshoots and undershoots near steep gradients to within some error tolerance. It turns out that it is cost effective to relax the monotonic solution requirement in this fashion. The values of (n), (m), (μ) and (K) required to satisfy the error tolerance to any selected value depends upon the structure of the noise waves. The structure of the noise waves depends upon the noise properties of a prospective convective algorithm for various values of the Courant number and the nature of the steep gradients which are to be simulated with the algorithm. Attempts to determine by analysis the proper values of (n), (m), (μ) and (K) for the adequate control of computational noise in the convective solutions of simple linear and nonlinear waves by the italicized fourth and higher order algorithms of Section 1 have failed due to the complexity of the problem. Consequently, empirical tests are used to establish the magnitudes of these constants. A discussion of these data is provided in Section 3.

3. Comparison of Numerical Experiments

Numerical experiments are now discussed which involve the application of the italicized fourth and higher order convective algorithms of Section 1 with and without the use of the filter defined in Section 2 for two sets of test problems. The reversible Boris–Book and Fromm monotonic algorithms are also applied to these test problems. One set of test problems is linear and the other set is nonlinear. These sets of test problems are generated by setting the convective velocity, u, equal to either 1 or $\omega/2$ in Eq. (1) and by choosing a range of initial conditions. The initial conditions for the linear wave propagation problems included the distributions that were Guassian-shaped, roof-shaped, and roof-shaped with round corners, and these distributions with broad tops. Examples of a roof-shaped and a Guassian-shaped distribution with broad tops are shown in Figs. 1 and 3, respectively, with the solid lines. Steep gradient wavelengths of 2, 4, 6, 8, 10, 12, 24, and 48 mesh intervals are simulated in order to investigate the noise and accuracy properties of the solutions. The illustrated results are for the short wavelength steep gradient distributions. Some discussion of the properties of the longer wavelength solutions is also provided.

In the illustrated results for the linear test problems, the initial distributions of the mesh function ω are designated by solid lines. These distributions are also the exact solutions which are displayed 60 mesh intervals to the right of the initial distribution location. The approximate solutions by the various convective algorithms which are designated along the left ordinate in the figures are indicated by a dot for the function value at each mesh point. Most of the displayed results

are featured at a Courant number of $\frac{1}{10}$, with the computations performed for 600 time cycles. At this Courant number, the errors from the time differencing are negligible compared to the space derivative errors. This condition is useful in making comparisons of the space derivative errors of the various solution algorithms. Other Courant numbers used in the linear wave problems are 0.9, 0.8, 0.75, 0.6, 0.45, 0.4, 0.3, 0.15, and 0.05 in order to investigate time-differencing errors and stability. Some comments on the properties of the solution algorithms at Courant numbers other than $\frac{1}{10}$ are provided later.

The initial conditions for the nonlinear test problems are a ramp distribution immersed in uniform distributions. The ramp distribution sloping downward to the right constitutes a compression wave initial condition. The ramp distribution sloping upward to the right is for an expansion wave initial condition. The initial distribution of the ramp is two mesh intervals in these two nonlinear test problems.

The approximate solutions displayed in Figs. 1–6 were carried out without the application of the filter of Section 2. In Figs. 1 and 2, the steep gradient regions are distributed over too few mesh points to allow smooth solutions. Figures 3

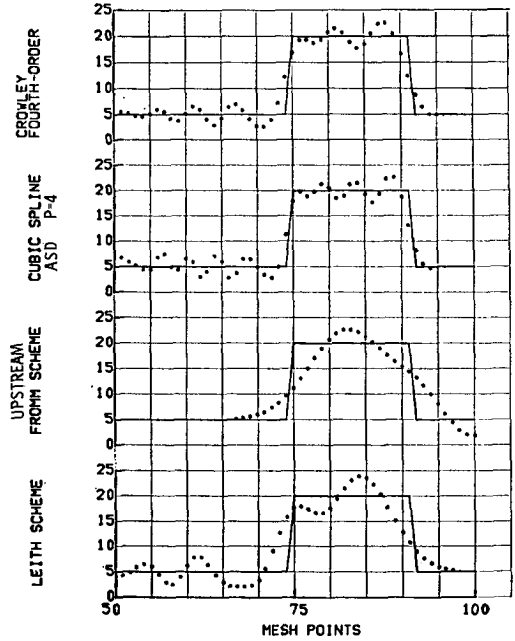

FIG. 1. The dots indicate the numerical representation of the linear wave shown which has been propagated 60 mesh intervals with 600 time cycles by a second, second, sixth, and fourth order convective scheme. Note the significant increase in the frequency of the computational noise as the order of the convective scheme is increased. $\sigma = 0.1$; exact solution (——); approximate solution (····).

and 4 show that by moderating the steep gradients of Figs. 1 and 2, the errors between the computed and exact solutions are impressively reduced for the Crowley and the cubic splined ASD computations. The improvement in the second order algorithms is less dramatic. The errors between the exact solution and computations with the second order methods can be reduced to the level of the Crowley method by more than doubling the number of mesh points over which the ramps and the corners of the ramps are distributed.

Computations show that steep gradient regions and the corners connecting them to shallow gradient regions can always be distributed over a sufficient number of mesh points so that no noise waves are excited in the convective computations of any order accuracy for linear wave propagation. Also, the higher the order of accuracy of the convective algorithm, the less the steep gradients have to be moderated to prevent excitation of the noise waves. Associated with this fact is that the noise waves are of higher frequency and lower amplitude as the order of accuracy of a given type of convective algorithm is increased. Finally, the amplitude but not the frequency of the noise waves is reduced as the steep gradient region is moderated for linear wave modeling. These various effects are illustrated in the data shown in Figs. 1–5 at a Courant number of $\frac{1}{10}$.

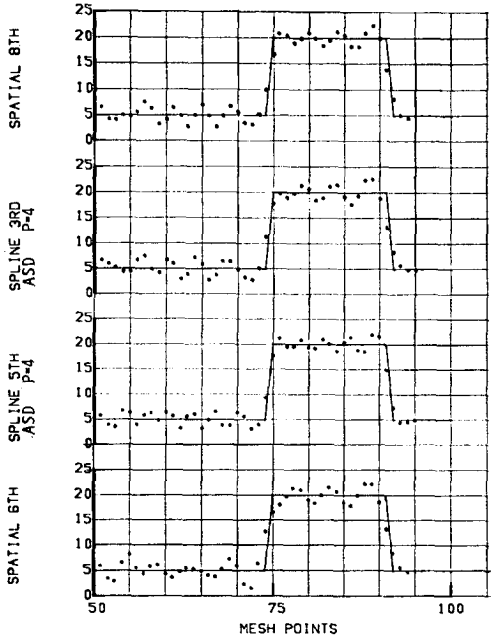

FIG. 2. Same as the comments in Fig. 1, except for sixth, tenth, sixth, and eight order schemes.

From Figs. 1–5, the wavelengths of the noise waves are taken to be shorter than eight, six, and four mesh intervals for fourth, sixth, and above eighth order

[redacted]

the values of (n) may have to be larger. To illustrate this trend, compare Figs. 2 and 6. Figure 6 illustrates the noise properties of several convective algorithms at a Courant number of 0.8. Note the dramatic gain in the wavelength of the computational noise of the algorithms with Crank–Nicholson time differencing. To compensate for this increased wavelength, it has been found that (n) must be 4 for spatially fourth or higher order convective algorithms with Crank–Nicholson time-differencing in the range of Courant number from about $\frac{1}{3}$ through $\frac{4}{5}$. The cubic and quintic splined ASD methods with P equal to 4 or 3 require (n) to be 4 and 3, respectively, in this range of Courant number. The Fromm one-flux and the Fromm two-flux schemes require (n) to be 4 between a Courant number

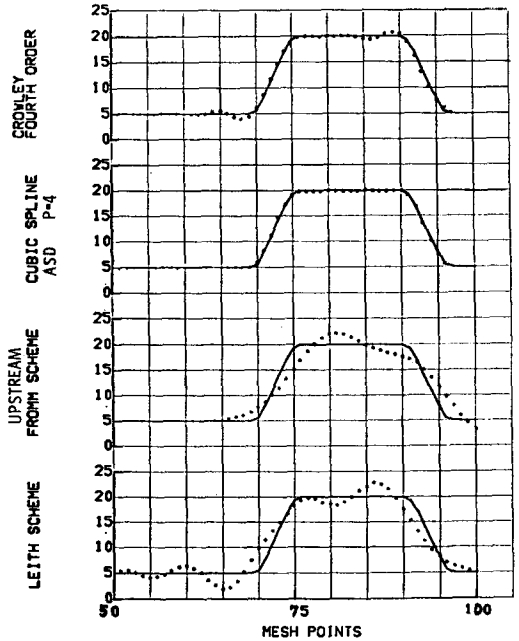

FIG. 3. Same as the comments in Fig. 1 with the following additional consideration. Compare Fig. 1 with Fig. 3 and note the significant increase in the amplitude but not the frequency of the computational noise by decreasing the number of mesh intervals over which the steep gradient regions are distributed.

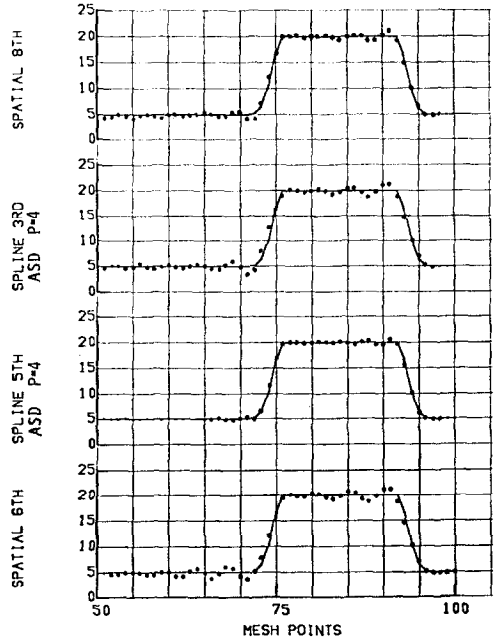

FIG. 4. Same as the comments in Fig. 2 with the same additional comment as in Fig. 3, except compare Fig. 2 with 4.

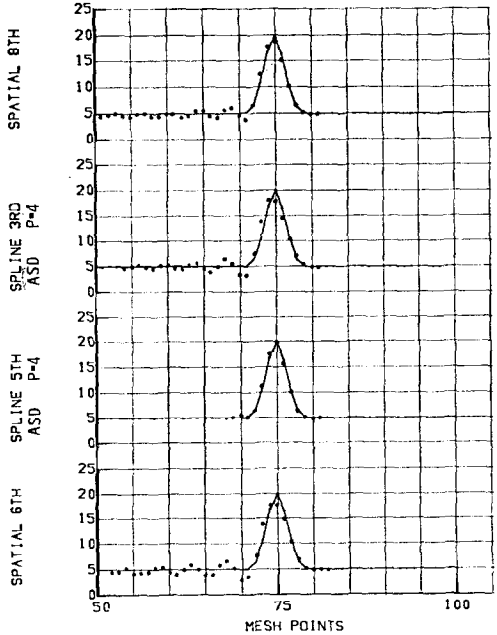

FIG. 5. Same as the comments in Fig. 2 with the same additional comment as in Fig. 3, except compare Figs. 4 and 5.

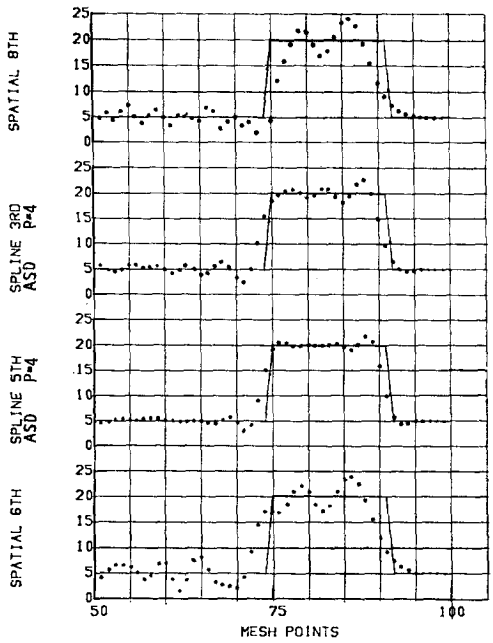

FIG. 6. Same as the comments in Fig. 2 except for 75 time cycles. Compare Fig. 2 with 6 and note the reduction in frequency of the computational noise associated with the increase in the Courant number. $\sigma = 0.8$.

of about $\frac{1}{3}$ and $\frac{1}{2}$. These schemes require an (n) of 5 for Courant numbers greater than about $\frac{1}{2}$ and less than about $\frac{9}{10}$. The values of (n) recommended for these Fromm schemes also are applicable to the Crowley scheme.

Using the values of (n) and (m) defined above for these various convective schemes, computations shown in Figs. 7–12 are performed with the designated convective schemes. The fourth and higher order accurate schemes are filtered by the method defined in Section 2 for (μ) equal to $\frac{1}{10}$ and K equal to 1. A comparison of Figs. 2 and 9 and Figs. 5, 10, and 11 illustrate the power of the filter to remove the computational noise from the solutions without inflicting large losses in the amplitude response of sharply peaked waves. Figures 10 and 12 show the large loss in amplitude response of sharply peaked waves produced by the reversible Boris–Book algorithm. The Fromm monotonic algorithm inflicts almost this much loss in amplitude accuracy. Even for propagation of a linear Guassian wave with a wavelength of 48 mesh points for a 60 mesh interval propagation at Courant numbers of $\frac{1}{10}$, $\frac{2}{5}$, and $\frac{4}{5}$, the errors in the amplitude of the extremum are about 6, 4, and $\frac{1}{2}$%, respectively, with the reversible Boris–Book

algorithm and about 5, 3, and 2%, respectively, for the Fromm monotonic algorithm. The Crowley fourth order scheme is estimated to require about a 16 mesh point Guassian distribution to achieve errors in the amplitude of the extremum of less than about 5, 2, and $\frac{1}{2}$% for Courant numbers of $\frac{1}{10}$, $\frac{2}{5}$, and $\frac{4}{5}$, respectively. The cubic splined ASD method achieves errors of less than 1% in the amplitude of the extremum of a 12 mesh point Guassian distribution for these three Courant numbers. For Courant numbers about $\frac{1}{10}$ or less, the estimated errors of the amplitude of the extremum are less than about 5% for Guassian distributions about 10 and 7 mesh points wide for a 60 mesh interval propagation with cubic and quintic splined ASD algorithms, respectively. Thus, the monotonic second order algorithms require at least three times more mesh points to simulate linear peaked waves to the same level of accuracy of the extremum as that required by the filtered fourth and higher order accurate convection algorithms.

The phase-error properties of the various fourth and higher order convective difference schemes tested at small Courant numbers are excellent except for short wavelength waves. The application of the filter of Section 2 reduces these short wavelength phase errors as a comparison of Fig. 2 with 9 indicates. A comparison

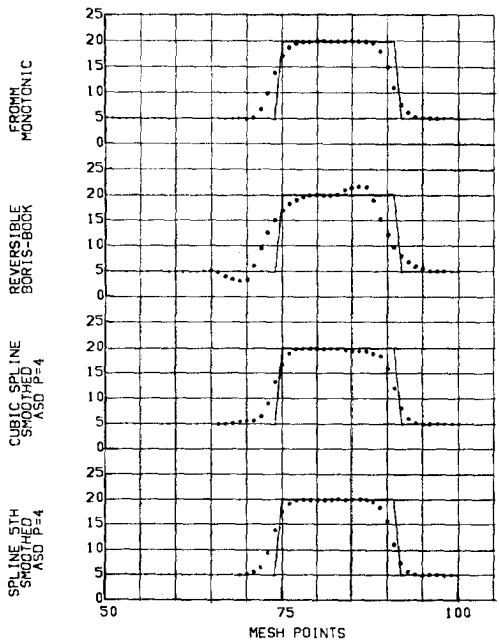

FIG. 7. The same test computation as shown in Fig. 6 except the application of the filter of Section 2 has been used to remove the computational noise in the splined ASD convective schemes. $\sigma = 0.8$; filter constants: $c = 0.1$; $K = 1$.

of Fig. 6 with 7 shows that the application of the filter of Section 2 also reduces the short wavelength phase errors at a Courant number of $\frac{4}{5}$. The phase-error properties of the filtered fourth and higher order convective difference schemes are as good as or better than the Fromm monotonic scheme for short wavelength simulations as the examination of Figs. 7 and 8 show for Courant numbers of $\frac{2}{5}$ and $\frac{4}{5}$. The reversible Boris–Book scheme yields somewhat better phase-error properties than the other filtered schemes tested only in the range of Courant numbers between $\frac{1}{4}$ and $\frac{1}{2}$ for the propagation of short wavelength linear waves. For Courant numbers greater than about $\frac{1}{2}$, the reversible Boris–Book scheme is not competitive with the other filtered convective difference schemes in phase-error accuracy for the propagation of short wavelength linear waves.

In modeling the two nonlinear problems, a staggered mesh is used for the velocity term in the Fromm monotonic, the Fromm one-flux, the Fromm two-flux and the reversible Boris–Book convective algorithms. The staggered mesh values of velocity are obtained by a simple linear interpolation of the values of the adjoining mesh points. No staggered mesh is used in the computations with spatial fourth and the cubic splined ASD method with (P) equal to 3. The simple expansion wave problem is simulated by these various convective algorithms with the filter of Section 2 applied for Courant numbers of 0.15, 0.45, and 0.9. (μ) is

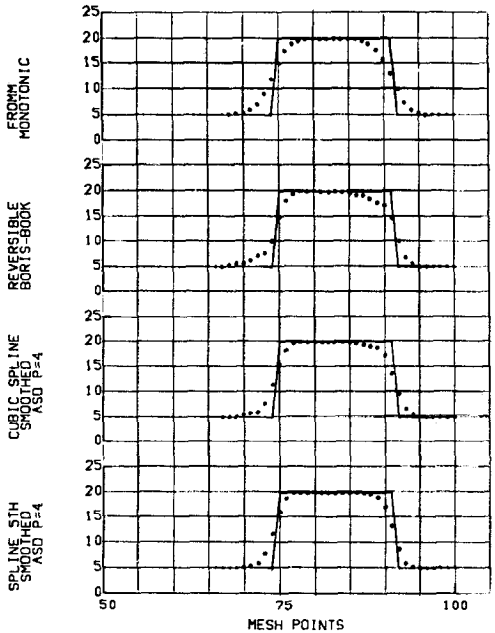

FIG. 8. $\sigma = 0.4$. Filter constants: $c = 0.1$; $K = 1$.

set to $\frac{1}{10}$ and K is 1. The computational noise generated by the steep gradient initial condition is successfully suppressed. After the expansion wave solutions have propagated several mesh intervals or more, the disagreement between the various solutions tends to reduce. After the expansion wave solutions have propagated many mesh intervals, the disagreement between the various solution tends to vanish except in the corners of the ramp wave. The reversible Boris–Book algorithm and the cubic splined ASD method provided sharper corners than do the other convective difference schemes tested. The Fromm one-flux and the Fromm two-flux schemes yielded anomalous results at a Courant number of 0.9.

and higher order convective algorithms for shock propagations of 60 mesh intervals at Courant numbers of 0.15, 0.45, and 0.9. Without the aid of the filter of Section 2, the solutions in a few time cycles from the start tend toward either precipitous

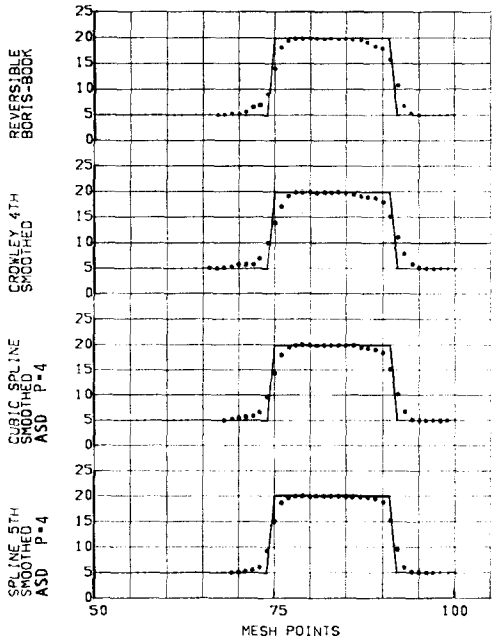

FIG. 9. The comparison of Figs. 7, 8, and 9 shows that the phase errors of the Fromm monotonic and filtered splined ASD methods are reduced as the Courant number is reduced. However, the acuity of the steep gradient regions improves upon reducing the Courant number for filtered splined ASD computations, whereas the opposite result occurs in the Fromm monotonic scheme. Notice the fine results of the Boris–Book scheme for the Courant number range represented in Figs. 8 and 9. A comparison of the results of Leith's scheme in Fig. 1 with the results of Boris–Book scheme in Fig. 9 shows dramatically the power of the Boris–Book filter to improve the solution accuracy in phase and amplitude properties. $\sigma = 0.1$. Filter constants: $c = 0.1$; $K = 1$.

instability or wildly varying values of the dependent variable rapidly moving downstream from the shock location to an observer riding the shock. The application of the filter of Section 2 in conjunction with these various convective algorithms eliminates the computational noise from these shock solutions if the appropriate choices of (μ) and K are used. The monotonic shock solution widths extend about two mesh intervals with a small amount of rounding of the downstream corner of the shock solution. The reversible Boris–Book scheme yielded solutions with shock widths of about two mesh intervals for Courant numbers of 0.15 and 0.45. This algorithm yields anomalous solutions for the case with a Courant number of 0.9. The Fromm monotonic scheme yielded solutions with shock widths of about one and one-half mesh widths for Courant numbers of 0.45 and 0.9. This algorithm yielded solutions with shock widths of about two mesh intervals for a Courant number of 0.15. The shock speed errors for a Courant number of 0.15 are estimated at about 0.02% for the reversible Boris–Book, the filtered spatial fourth, and the filtered cubic splined ASD method with (P) equal to 3. The shock

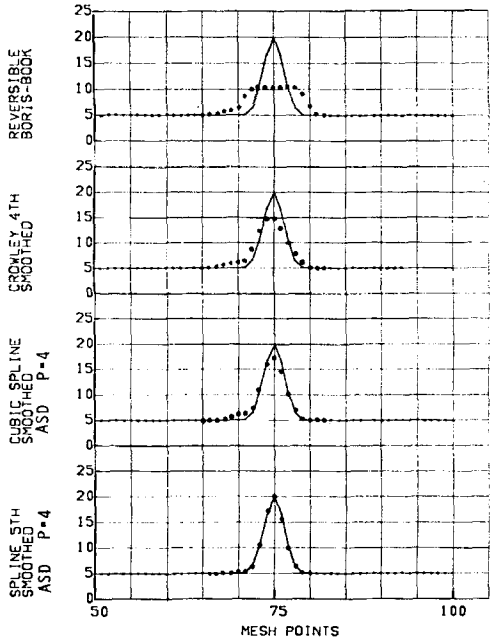

FIG. 10. The Guassion wave distribution is propagated 60 mesh intervals for 600 time cycles. Note the excellent phase but poor amplitude properties of the Boris–Book algorithm for this problem. Also note the substantial improvement in amplitude response as the order of the filtered algorithms is increased. Compare Figs. 5 and 10 and observe the small amount of amplitude damping of the peak of the wave which the filter of Section 2 produces. $\sigma = 0.1$. Filter constants: $c = 0.1$; $K = 1$.

speed errors of the other schemes tested are estimated to be about five times larger. The shock speed errors increase as the Courant number is increased for all the filtered convective schemes tested with no scheme dramatically more accurate than the others at a Courant number of 0.45.

The computational cost associated with the use of the filter of Section 2 is related to the size of the average value of K over many computational time cycles or simply $\bar{K}$. The larger the value of (μ) selected, the smaller the value of $\bar{K}$ required to control the oscillations from the computational noise to some selected error tolerance. Steep gradient regions are spread over more mesh intervals as (μ) increases in size particularly in the range of (μ) of $\frac{1}{4}$ to $\frac{1}{3}$.

To maximize computational accuracy in steep gradient regions, it is necessary to minimize (μ). To maximize computational efficiency it is necessary to minimize both (μ) and $\bar{K}$. In order to attempt to assess the optimum (μ) and $\bar{K}$ with respect to Courant number for each algorithm tested, the computations of the linear and nonlinear test problems defined above are performed for values of (μ) of 0.002, 0.02, 0.1, 0.2, 0.25, and 0.333. Values of $\bar{K}$ are determined for computational noise whose oscillations are in error either less than one half of 1 % or 0 %. The reference level for the percent error calculation is the difference in the maximum

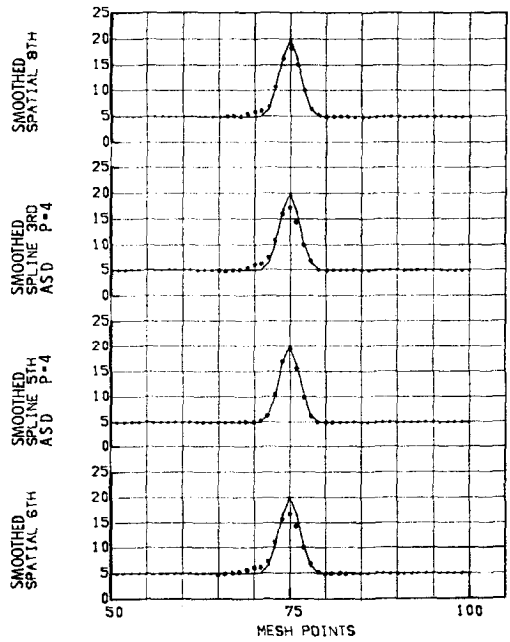

FIG. 11. Same as the comments in Fig. 10, except compare Figs. 5 and 11.

and minimum values of the required solution. These statistical data are summarized as follows.

The range of values of (μ) required to minimize $\overline{K}$ and minimize excessive diffusion by the action of Eq. (3) near steep gradients of the convective solution is found to be dependent upon the Courant number, the noise properties of the convective algorithm, and the stringency of the error tolerance of the allowed computational noise. The delineation of the optimum relationship of (μ) with Courant number to minimize $\overline{K}$, in each tested convective algorithm is determined to be impossible with the wide range of values of (μ) chosen. However, it is known that the proper range of (μ) in which this relationship should be developed is for (μ) between about $\frac{1}{10}$ and $\frac{1}{3}$. It is also known that (μ) must increase with the Courant number. Finally, the stringency of the error tolerance of the allowed computational noise has a decisive effect on the size of $\overline{K}$ required at Courant numbers greater than about $\frac{1}{3}$. For example, with the shock solutions performed with cubic splined ASD approximation with (P) equal to 3 for an error tolerance of one-half of 1 %, the required $\overline{K}$ values are about 1, 1, and 3 for Courant numbers of 0.15, 0.45, and 0.9, respectively, with a (μ) of $\frac{1}{5}$. This same computation per-

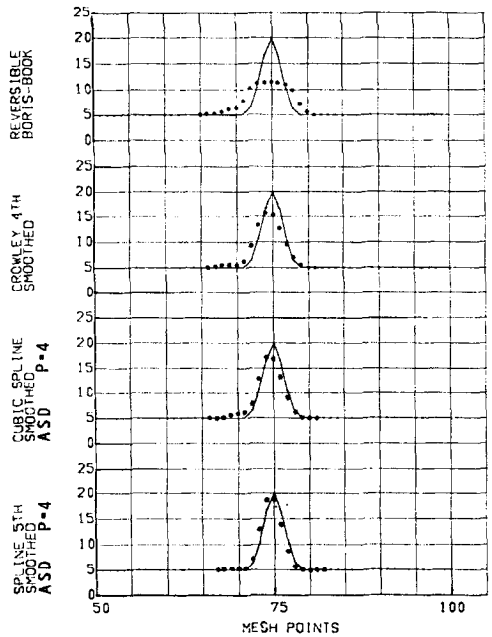

FIG. 12. Compare Figs. 11 and 12 and note the increase in phase errors of the various filtered solutions with increased Courant number. In spite of this, note the monotonic response of the solutions. $\sigma = 0.4$. Filter constants: $c = 0.1$; $K = 1$.

formed for an error tolerance of 0% requires $\bar{K}$ values of about 1, 2, and over 100 for Courant numbers of 0.15, 0.45, and 0.9, respectively, with (μ) of $\frac{1}{5}$. Similar dramatic increases in the required value of $\bar{K}$ with Courant number and with the stringency of the error tolerance for the shock solution with some of the other fourth and higher order convective algorithms are noted for a (μ) of $\frac{1}{5}$. Using values of (μ) of $\frac{1}{4}$ in these computations, the value of $\bar{K}$ required to satisfy the zero error tolerance drops sharply at the largest Courant number used. Unfortunately, the accuracy of computation of linear problems such as those shown in Figs. 7–12 are reduced by spreading the steep gradient regions over more mesh intervals than are necessary to achieve monotonic solutions. At a value of (μ) of $\frac{1}{5}$, the computations of linear problems such as those displayed in Figs. 7–12 are very modestly reduced in accuracy by spreading the steep gradient regions over slightly more mesh intervals than are necessary to achieve monotonic solutions.

The conclusion of the data collected thus far is that it is highly probable that for each convective algorithm an empirical relationship with respect to the Courant number can be developed which minimizes the size of (μ) and $\bar{K}$. While the development of such optimum relationships of (μ) with Courant number may be cost effective in certain applications, further elucidation of such relationships are not provided here. Rather, nonoptimized versions of the filter of Section 2 are recommended for general applications as follows.

(μ) should be set to $\frac{1}{5}$. The error tolerance of the computational noise should be selected between zero and several per cent error as desired by the user. The reference value for the error computation can be obtained by finding the magnitude of the difference the dependent variable across the steep gradient region from which the computational noise originates. The Courant number should be restricted below the values at which the value of $\bar{K}$ shows a dramatic increase in size compared with the required size of $\bar{K}$ for a small Courant number.

If the user desires a simpler procedure yet, the following recommendation is proposed. (μ) should be set to $\frac{1}{5}$. (K) should be set to 1 and 2 for local Courant numbers less than about $\frac{1}{2}$ and greater than $\frac{1}{2}$, respectively. While this latter recommended procedure may yield only "nearly monotonic" solutions of single

The following comments are offered to aid in justifying the selection of the design of the filtering technique of Section 2 compared with other candidate designs. A class of filtering techniques has been examined after the van Leer filtering concept, which involves truncation errors of higher than third order. Specifically, filters which involved second, third, fourth, and sixth divided differences of second divided differences were studied. The conclusion of this study is that without some nonlinear device like that presented in Section 2 for avoiding the application of the filter at sharply peaked waves, the sharp peak of the wave

always suffers a nontrivial loss in amplitude accuracy. The higher order filters are very complicated to implement to avoid this difficulty because the coupling of mesh point data occurs over very many mesh points. While the high order filters could be made to eliminate the gross effects of computational noise, small amplitude oscillations are generated in unexpected locations of the solution many mesh points from the steep gradient regions. The design of suitable nonlinear cutoff devices of these noise components may be possible, but no simple prescription for doing this has been found. As has been noted, the primary shortcoming of the Boris–Book and the van Leer computational noise filtering techniques is the large loss in amplitude accuracy incurred in the solution of sharply peaked waves. The filtering technique proposed in Section 2 is the simplest one discovered which avoids this shortcoming while preserving excellent steep gradient acuity.

The minimum cost associated with the use of the filter of Section 2 is less than or more than that required by the Boris–Book filtering technique depending upon the number and extent of the steep gradient regions simulated, the total number of computational mesh points used in the computational domain, the stringency of the error tolerance on the oscillations near the steep gradient regions, and the chosen size of the Courant number for the computation. The cost effectiveness of this filtering technique compared with that of the Boris–Book and van Leer techniques will be additionally dependent upon the efficiency of the fourth and higher order solution algorithms with which it is used and the nature of the steep gradients to be simulated. The assessment of these various complex factors must await further studies.

In applications where coupled-multivariable equations are solved simultaneously, the application of the filter of Section 2 must be made independently to each dependent variable each time cycle. Where nonorthogonal computational mesh structures are employed, conservative nonorthogonal variants of the filter of Section 2 may have to be developed.

Concluding Remarks

The simple test problems discussed show that the computational noise excited near steep gradient regions in discrete fourth and higher order solutions of simple linear and nonlinear hyperbolic waves can be removed by the proposed nonlinear filtering technique. The proposed filter reduces the phase errors of short wavelength distributions in the solution without inflicting substantial amplitude losses in sharply peaked waves. Used in conjunction with fourth and higher order convective difference schemes, it requires less than one-third the mesh points to model the extrema of sharply peaked waves to a given accuracy than are necessary for the filtered second order accurate convective difference schemes of Boris–Book

and van Leer. The relative computational cost of using this filtering technique is at present uncertain. Definitive quantitative assessment of the cost effectiveness of the proposed filtering technique must await further comparative studies in realistic flow simulations.

It is shown that sixth and tenth order accuracy respectively is achieved by the cubic and quintic splined ASD method for linear wave propagation problems at small Courant number computations. It is expected that the splined ASD algorithms with the proposed filter can be developed to integrate the convective/diffusive conservation equations in cartesian or transformed mesh system whether uniform or not. Further study of the application of the proposed filter to other fourth and higher order algorithms is also recommended.

ACKNOWLEDGMENT

I wish to express my gratitude to Harold Shniad for supplying his derivation of the odd-degree polynomial spline algorithm with coefficients for splines to degree 7. With his helpful aid, the splined ASD method was speedily implemented.

REFERENCES

1. J. C. WILSON, *J. Inst. Math. Appl.* **10** (1972), 238–257.
2. R. W. MACCORMACK, AIAA Paper 69–354, 1969.
3. J. E. FROMM, IBM Research Laboratory Report RJ732, 1970.
4. S. ORSZAG, *J. Fluid Mech.* **49** (1971), 75–112.
5. J. GAZDAG, *J. Computational Phys.* **13** (1973), 100–113.
6. J. E. FROMM AND F. H. HARLOW, *Phys. Fluids* **6** (1963), 975–982.
7. H. W. PATTERSON, C. K. FORESTER, AND J. E. BARTON, "Computer Program Manual Cryogenic Tank External Loop Pressurization Analysis," Contract NAS9-12977 for Propulsion and Power Systems, 5-2921, NASA LBJ Space Center, Houston, Tex., May 1973.
8. L. L. PRESLEY, "A Comparison of a Shock-Capturing Technique with Experimental Data for Three-Dimensional Internal Flows," NASA Ames Research Center, 1975.
9. J. P. BORIS AND D. L. BOOK, *J. Computational Phys.* **77** (1973), 38–69.
10. J. P. BORIS AND D. L. BOOK, "A Minimum Error Finite-Difference Technique Designed for Vector Solution of Fluid Equations," Naval Research Laboratory Report, 1974.
11. B. VAN LEER, *J. Computational Phys.* **14** (1974), 361–370.
12. J. E. FROMM, *Phys. Fluids Suppl. 2* **12** (1969), 3–12, 113–119.
13. S. A. ORSZAG AND L. W. JAYNE, *J. Computational Phys.* **14** (1974), 93–103.
14. W. P. CROWLEY, *Monthly Weather Rev.* **1** (1968), 1–11.
15. J. E. FROMM, *Phys. Fluids Suppl. 2* (1969).
16. J. E. FROMM, *Monthly Weather Rev.* **96** (1968), 573.
17. H. SHNIAD, private communication.
18. R. S. HIRSH, *J. Computational Phys.* **19** (1975), 90–109.